

Mini review

Electrochemical Techniques for the Detection of Cancer Cells and Cell-Surface Glycan Expression: A Mini Review

Feng Zhao, Cheng Cheng, Ning Xia *

Henan Province of Key Laboratory of New Optoelectronic Functional Materials, College of Chemistry and Chemical Engineering, Anyang Normal University, Anyang, Henan 455000, People's Republic of China

*E-mail: xianing82414@csu.edu.cn

Received: 20 April 2017 / *Accepted:* 15 June 2017 / *Published:* 12 July 2017

Developing novel methods for the detection of cancer cells and glycan expression on cell surface is urgently imperative. Electrochemical biosensors have attracted considerable attention for the detection of cancer cells in view of their sensitivity, simple in operation, rapid response, and compatibility with miniaturization. In this work, we focused on the recent progress in the development of electrochemical methods for the detection of cancer cells of lung, breast, colorectal liver, leukemia, cervical carcinoma, and burkitt's lymphoma. Also, the electrochemical techniques used for monitoring the glycan expression on cell surface were summarized.

Keywords: cancer cells; electrochemical techniques; cytosensors

1. INTRODUCTION

Cancer continues to threaten people's life and has been a major unmet challenge to healthcare. In United States, cancer has been the second most common cause of death next to heart disease in incidence [1]. Cancer emerges from our healthy tissues and displays many similarities with own tissues [2]. Reproduction of cancer cells in an uncontrolled manner complicated both diagnose and treatment of cancers. At present, most cancer-associated deaths were accounting from the metastasis of the cancer tumors, which presents a destructive damage to normal physiological function [3]. Early diagnosis is often essential for reducing the mortality rate from cancer although early stage recognition of cancers remains a big challenge [4]. Sensitive detection of tumor cells could provide an effective routine for monitoring progression of cancer. Thus, the construction of a biosensing platform capable of distinguishing a tumor cell from a normal one is always demanded for the molecular basis of cancer

level and for its early diagnosis.

So far, many attempts have been made for the detection of cancer cells and cell-surface glycan expression, including cytological testing, fluorescent imaging, magnetic resonance imaging, positron emission tomography, computerized tomography, X-ray, radiography and ultrasound [5]. However, most of these approaches suffer from high-cost and time-consuming in the experimental process or instrumentation. Moreover, some approaches are likely to bring on side effects including radioactive risk [6]. As a result, the development of novel methods for the detection of cancer cells is urgently imperative. Given their sensitivity, simple in operation, rapid response, and compatibility with miniaturization, electrochemical biosensors have attracted considerable attention for sensing of cancer cells [6]. Electrochemical cytosensors are usually fabricated based on a sandwich-like structure through the recognition of protein molecules expressed specifically on the targeted cancer cells. Aptamers, derived from systematic evolution of ligands by exponential enrichment (SELEX), have been the most used molecular probes in this recognition field [7, 8]. Considering their strong affinity to the receptors widely expressed on the targeted cancer cells, aptamers-based electrochemical cytosensors endowed with an excellent specificity and selectivity. Considering the overexpression of folate receptors in some cancer cells, several electrochemical cytosensors were demonstrated to detect cancerous cells via the high affinity of folic acids for their receptors. In this review, we will focus on the recent progress made in the development of electrochemical methods for the detection of cancer cells and cell-surface glycan expression. The analytical performances of various electrochemical techniques for the detection of different cancer cells were compared.

2. ELECTROCHEMICAL DETECTION OF CANCER CELLS

2.1 Human non-small-cell lung cancer cells

Among all cancers, lung cancer is the most prevalent neoplasm and accounts for about 25% of all cancer-related mortality in human beings [9]. Since lungs are mostly associated with the supply of oxygen, lung cancer patients are always suffering from reduced oxygenation levels and a higher incidence of metastasis [10]. Like to many other cancers, lung cancer is difficult to be diagnosed at an earlier stage because many symptoms including shortness of breath, coughing, and weight loss do not emerge in its early course, leading to unfavorable treatment [11]. Lung cancer mainly consists of small cell lung carcinoma (SCLC) and nonsmall cell lung carcinoma (NSCLC) [10]. Of the two most common types of lung cancer, NSCLC accounts for approximately 80% of the lung malignancies. SCLC usually responds poorly to chemotherapy and radiation therapy and exhibits a lower survival rate. However, the five year survival rate could be increased to 60% from 20% if NSCLC is diagnosed in the stage I [12].

Shim and coworkers designed an aptamer-based amperometric nanobiosensor for A549 human non-small-cell lung cancer cells detection [13]. Since mucin-1 (MUC1) glycoproteins expressed on the surface of A549 cells, the specific aptamer S1 conjugated a conducting polymer nanocomposite was utilized as a recognition probe for targeted cells binding, where the MUC-1 aptamer was covalently attached on a conducting polymer-Au nanoparticles (AuNPs) composite layer polymerized with TTBA

on AuNPs with the aid of hydrazine sulfate. In the presence of A549 cells, further biocognition with aptamer-modified AuNPs labeled with hydrazine sulfate (aptamer/AuNPs/hydrazine) was carried out. In this case, an amplified electrochemical signal was generated due to the catalytic reduction of hydrogen peroxide mediated by the biocognition materials. Through measuring the catalytic signal of H_2O_2 or the silver deposition proportional to the amount of targeted cells, A549 cells with concentration ranging from 15 to 10^6 cells/mL were detected with a detection limit of 8 cells/mL.

With the excellent conductivity of multiwalled carbon nanotube (MWCNT) and AuNPs, Zhang and coworkers reported the competitive detection of glycan expression with mannose as a model. First, AuNPs-modified glass electrode was functionalized by thiomannosyl, which allowed for the attachment of HRP/Con A-functionalized MWCNT. The electrochemical signal was measured by monitoring the catalytic reaction of HRP toward the oxidation of hydroquinone (QH_2) by H_2O_2 . However, the competitive interaction of mannose on the surface of lung cancer cell A549, liver cancer cell QGY-7703 or prostate cancer cell LNCaP with that on the electrode surface prevented the attachment of HRP/Con A-functionalized MWCNT, thus decreasing the catalytic current [14]. Furthermore, they prepared the thionine-bridged multiwalled carbon nanotube/AuNPs (MWCNT/Th/AuNPs) to realize the glycan assay on living cancer cells. The negatively charged AuNPs were attached to the anionic MWCNT surface with thionine acting as the linker. In this composite, thionine works as an electron mediator for the enzymatic signal amplification. This biosensor offered great promise for the analysis of other glycans on living cells, such as human liver and prostate cancer cells [15].

2.2 Breast cancer cells

Breast cancer has been the second common kind of cancer behind lung cancer and the most common kind of malignant tumor in women which often presents in the inner lining of the milk ducts or lobules [16]. Furthermore, a younger median age tend to be diagnosed for breast cancer in comparison with other common cancers [17]. For breast cancer cells detection, human MUC1 and carcino embryonic antigen (CEA) are the most used markers for electrochemical recognition. MUC1 has been demonstrated to be highly overexpressed in the surface of breast cancer cells, and is widely relevant to a poor prognosis and lymph node metastases increasement [18]. The expression level of CEA has a positive correlation with the therapeutic response in patients with breast cancer [19].

Li et al. demonstrated a novel accurate and special detection of breast cancer cells based on two tumor markers expressed on the cell surfaces [16]. For the sensor fabrication, human MUC1 specific aptamer molecules were firstly immobilized on the surface of the gold working electrode. Then, the breast cancer cells were captured by the aptamer-modified electrode via the specific strong-affinity of MUC1 on the cell surface to the aptamer molecules, followed by the capture of CdS nanoparticles (CdS NPs) modified anti-CEA due to the overexpression of carcinoembryonic antigen (CEA) on the cell surface. The released amount of Cd^{2+} from CdS NPs through an acid-dissolution step was proportional to cancer cells. By measuring the voltammetric peak signal, breast cancer cells with a concentration ranging from 10^4 to 10^7 cell/mL could be monitored with a low detection limit. Additionally, by virtue of the two co-expressing tumor markers, satisfactory accuracy and selectivity

toward cancer cells detection were obtained. Moreover, Zhu and coworkers presented a competitive electrochemical method for the detection of cancer cells with aptamer-quantum dots (Apt-Qdots) conjugates as the recognition elements. The Apt-Qdots could be captured by the complementary DNA (cDNA) immobilized on the gold electrode surface. However, the competing interaction between Apt-Qdots and target cells to bind with cDNA led to the release of the Apt-Qdots. By measuring the electrochemical stripping peak of Cd^{2+} ions, the target cells could be determined in the range of $10^2 \sim 10^6$ cells/mL [20]. The aptamer-covered magnetic beads show high affinity and specificity for separation of target cells. Lv et al. demonstrated that the MCF-7 cells could be collected by aptamer-covered magnetic beads through the interaction between aptamer and MUC1 protein overexpressed on the cell surface. The captured cells were then recognized by DNA aptamers-capped CdS or PbS nanocrystals with ASV technology to quantify the dissolved Ca^{2+} or Pb^{2+} ions [21]. The method allowed for the detection of cancer cells down to 100 cells/mL. Meanwhile, Hua et al. demonstrated that the nucleolin aptamer AS1411-modified CdTe QDs coated on the surfaces of monodispersed SiO_2 NPs could be used to recognize the collected cells through the interaction of AS1411 aptamer and the nucleolin protein overexpressed on the cells surface. This allowed for the readout of cell concentration based on the stripping signal of CdTe using SWV assay [22].

Zuo and coworkers designed a multibranching hybridization chain reaction (mHCR) for the simple, sensitive and specific detection of four cancer cells (Figure 1) [23]. By virtue of mHCR, multibranching long products with multiple biotin and multiple branching arms could be obtained. Multiple horseradish peroxidase was attached for signal amplification via the conjugation of avidin. Additionally, the multiple branching arms were served as the binding sites for assembling on the surface of DNA nanostructured gold electrode. After introduction of targeted cancer cells, mHCR products could conjugate with cells through the specific interaction of aptamer and their receptors. Therefore, the cancer cells could be attached on the surface of DNA tetrahedral probes modified electrode through multivalent binding. An amplified electrochemical signal was obtained due to the catalytic reaction induced by HRPs rich in the mHCR products, which endowed the electrochemical sensor for cancer cells detection with high sensitivity and as few as four MCF-7 cells could be detected. Zheng and coworkers demonstrated a cytosensor for human breast cancer MCF-7 cells detection based on rolling circle amplification (RCA) reaction triggered enzyme-catalyzed polymerization [24]. A multifunctional hairpin structure DNA was designed with five fragments, that is, a short T linker, a cancer-specific aptamer sequence, a short T linker and a short sequence complementary to the C fragment. The attachment of cancer cells to the working electrode leads to the conformational alternation of thiol labeled DNA through the recognition ability of the aptamer SYL3C to their protein receptors epithelial cell adhesion overexpressed on the targeted cell surface. The conformational reorganization of DNA initiated RCA, resulting in a large amount of HRP-tagged DNA duplex assembled on the electrode surface through the biotin-streptavidin interaction. An amplified electrochemical signal could be obtained based on the polymerization of aniline to PANI around the DNA duplex catalyzed by HRP, which could accelerate effectively the electron transfer of $[\text{Fe}(\text{CN})_6]^{3-/4-}$. A lower detection limit of 12 MCF-7 cells/mL was obtained.

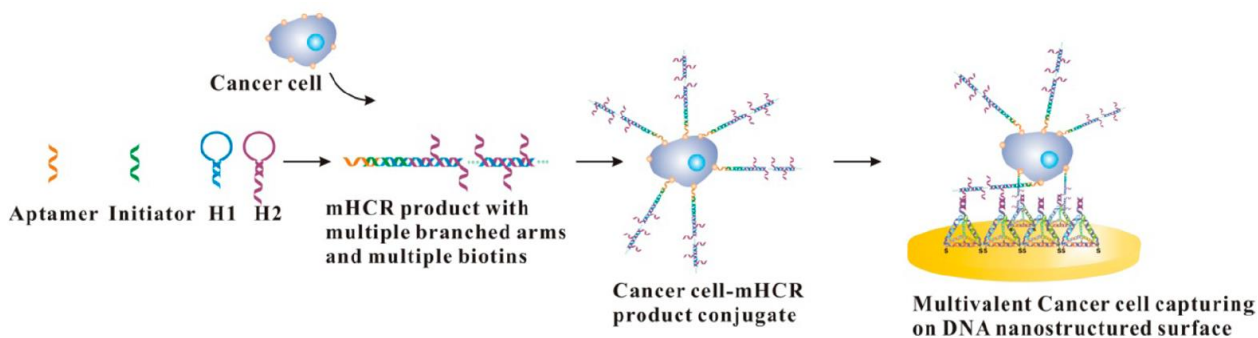


Figure 1. Multibranching HCR (mHCR) reaction was employed to synthesize long products with multiple biotin labels and multiple branched arms. After the conjugation of cancer cells and mHCR products, the cancer cells can be attached on the DNA nanostructured surface through multivalent binding. A large number of HRP s were attached on the mHCR products to amplify the electrochemical signal through enzyme catalytic reaction, which increased the detection sensitivity. Reprinted with permission from reference [23]. Copyright 2014 American Chemical Society.

Moreover, Yang and coworkers developed an antibody-aptamer electrochemical method for the detection of MCF-7 cells. In this work, the target cells were captured by antibodies, and then reacted with a DNA strand containing a MUC1 aptamer and a template C_{12} . The aptamer segment was used to recognize the captured cells and the template segment was used for the synthesis of Ag-NCs. Deposition of metal silver on Ag-NCs caused an amplified voltammetric signal, which was measured by SWV. The current is logarithmically related to the concentration of MCF-7 cancer cells with a detection limit of 50 cells/mL [25]. Recently, Zhu's group presented a general electrochemical platform for determination of cell glycan based on the cell-aptamer interaction and the ConA-modified AuNPs for both glycan recognition and signal amplification. After separation by MUC1-functionalized MBs, the target cells were conjugated with ConA-modified AuNPs. The captured nanoprobe catalyzed silver enhancement, which could be monitored by electrochemical analytical analysis [26].

2.3 Colorectal cancer cells

Colorectal cancer (CRC) is the third most common cancer in the worldwide, which causes greater than 10% death of all cancer mortalities [27]. Additionally, the fatality rate is approximately 40–50% for the patients suffered from CRC [27]. The number of people diagnosed with CRC continued to increase in many countries [28]. Even though there still exist many challenges in curing CRC patients, the overall survival rates are improved from a median of 10 months to more than 20 months due to the major advances in surgical and staging techniques over the last 20 years [29]. The availability of molecularly targeted therapies plays a vital importance with predictive tumour biomarkers as targeted recognition elements. Therefore, development of new methods based on the biomarkers associated with CRC is instantly required.

Recently, Hashkavayia et al. developed an electrochemical aptasensor based on an universal sandwich-like geometry for CT26 cancer cells detection [30]. For colorectal cancer cells assay, SBA-

15-3-aminopropyltriethoxysilane (SBA-15-pr-NH₂) and Au nanoparticles (AuNPs) were sequentially self-assembled on the surface of graphite screen printed electrode (GSPE), followed by labeled with thiol modified aptamer molecules. The nanostructured GSPE could serve as a nanoscale anchorage substrate for grabbing targeted cells. Afterwards, a sandwich structured biosensor formed with further treatment of cancer cells with aptamer molecules. According to the cyclic voltammetry and electrochemical impedance spectroscopy, CT26 cells with concentration from 10 to 6.0×10^6 cells/mL could be identified using the fabricated sensor and a detection limit of 2 cells/mL could be achieved. Considering the specificity of 5TR1 aptamer, the electrochemical sensor displayed a selective detection toward CT26 cancer cells even in the presence of a large number of control cancer cells.

2.4 Liver cancer cells

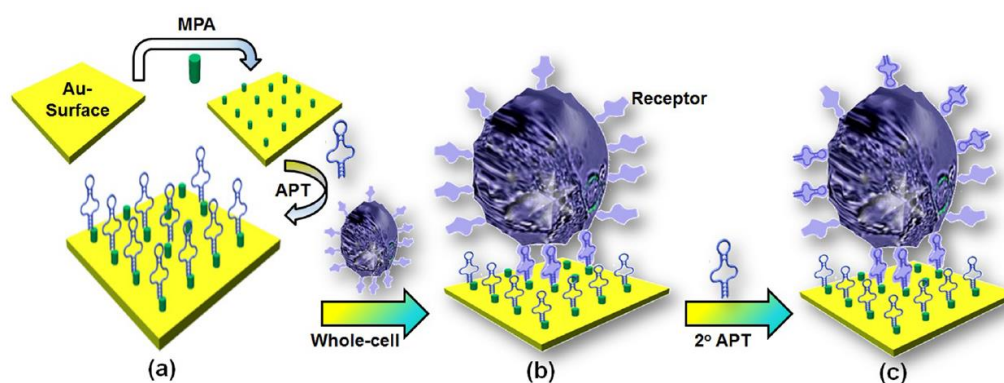


Figure 2. (a) TLS11a Aptamer Conjugated Au Surface via Coupling of Amino-Labeled Aptamer to the MPA–Au Surface; (b) Interaction of HepG2 Cells on Au Surface-Immobilized Aptamer; (c) Binding of Secondary Aptamer to Complete the HepG2 Cells Sandwich Format. Reprinted with permission from reference [31]. Copyright 2014 American Chemical Society.

Liver cancer is one of the most prevalent kind of lethal cancers which always arise from long-standing exposure to hepatitis B virus and hepatitis C virus or suffering from chronic liver diseases [32]. For patients diagnosed with early cancers, using surgical tumor resection or liver transplantation approaches generated many possibilities of recovery from cancers [33]. Unfortunately, most of the liver cancers patients are diagnosed at an advanced stage. In this case, no effective therapies could be carried out. Given the carcinogenesis process usually takes a long period of time, the development of novel screening methodologies for detecting the liver cancer in an early stage provides a window of alternative for patient survival.

Tiwari and coworkers developed an electrochemical biosensor for the label-free detection of HepG2 hepatocellular carcinoma cells using TLS11a aptamer molecules for targeted cells capture (Figure 2) [31]. Amino-labeled TLS11a molecules were assembled onto the surface of carboxylic acid modified gold electrode for HepG2 cells binding. After HepG2 cells attachment, further treatment with secondary TLS11a aptamer leads to a sandwich-like architecture. Since electrochemical impedance spectroscopy (EIS) was sensitive for the electrode surface modification, the presence of HepG2 cells could restrict the interfacial electron transfer speed through the working electrode. Furthermore, the

attachment of secondary TLS11a aptamer contributed to further resistance of electron transfer. The negatively charge of the cells and aptamer resulted in an electrostatic repulsion which blocked the access of the anionic probe to the electrode surface.

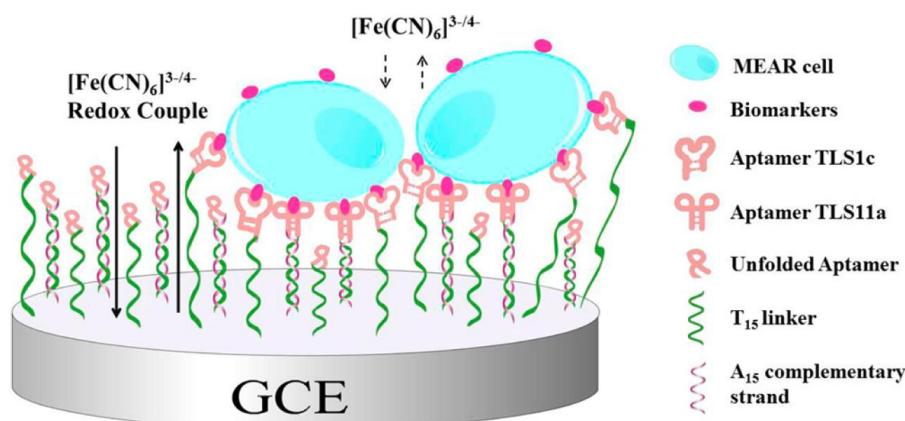


Figure 3. Scheme showing the designed ss-TLS1c/ds-TLS11a dual modified electrode for specific and sensitive detection of MEAR tumor cells. In this system, two MEAR cell-specific aptamers, TLS11a and TLS1c, are conjugated to the surface of GCE via a rigid dsDNA linker (T15/A15) and a flexible ssDNA linker (T15), respectively. Such a design could allow the most effective recognition of tumor cells by the GCE sensing surface. The specific binding of the cells to the modified electrode would bring a dramatic steric hindrance effect on the electron transfer of the redox couple $[\text{Fe}(\text{CN})_6]^{3-/4-}$ through the GCE, while the electrostatic repulsion between negative charges of the cell surface and the $[\text{Fe}(\text{CN})_6]^{3-/4-}$ may further inhibit the electron transfer, thus significantly reducing the electron transfer speed. Reprinted with permission from reference [34]. Copyright 2014 American Chemical Society.

Thus, an ultrahigh-sensitive EIS detection platform for HepG2 cells detection was achieved. The obtained sensor displayed an excellent detection range from 10^2 to 10^6 cells/mL with a detection limit of 2 cells/mL. Meanwhile, Qu et al. fabricated an electrochemical biosensor with two cell-specific aptamers (TLS1c and TLS11a) of MEAR cancer cells (Figure 3) [34]. The dual-modified electrode shows significant improvement in the sensitivity in contrast to the single aptamer (ds-TLS1c or ds-TLS11a) modified electrode. This method allowed for the detection of 5 MEAR cells in 10^9 whole blood cells.

2.5 Leukemia cells

As a common fatal cancer of blood cells, leukemia is accompanied by some symptoms including bleeding and bruising problems, the bones or joints pains, feeling weak, fever or night sweat, and frequent infections [35]. Because of high numbers of abnormal white blood cells, leukemia patients suffer from a lack of normal blood cells. The exact cause of leukemia continues to be an unsolved challenge. Currently, most of leukemia patients are treated with chemotherapy and radiation therapy. However, the innate and acquired resistance has been a major obstacle for leukemia treatment

[36, 37]. As a result, it is urgent to develop novel technologies for determining the type of leukemia and the stage for the acute therapy of leukemia.

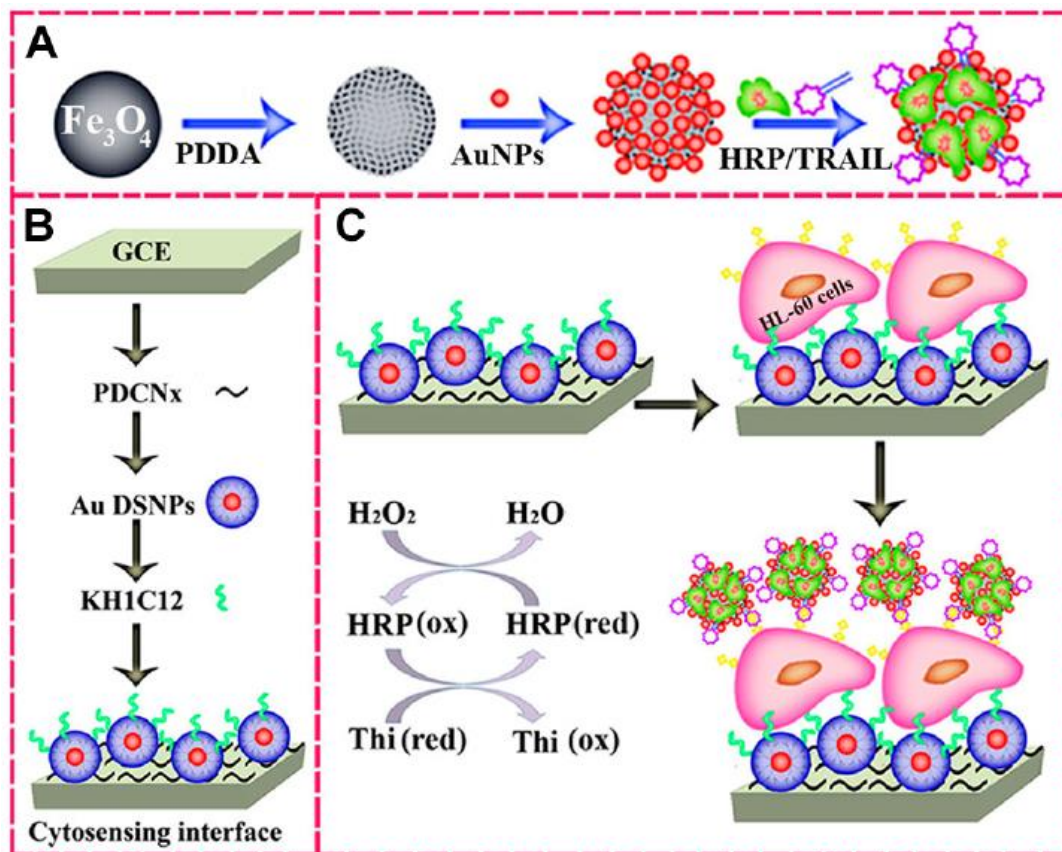


Figure 4. Schemes of (A) fabrication of HRP-TRAIL- Fe_3O_4 @Au hybrid nanoprobe, (B) assembly of the electrode interface, and (C) sandwich-like nanoarchitected electrode geometry for the cytosensing of HL-60 cells. Reprinted with permission from reference [36]. Copyright 2013 American Chemical Society.

Zheng et al. developed a novel nanobiotechnology-based electrochemical cytosensor for both selective detection of leukemia cells and quantitative evaluation of death receptor expression on the cell surfaces (Figure 4) [36]. The electrochemical detection platform majorly consisted of two components, namely, the nanoarchitected materials modified electrode and multifunctional hybrid nanoprobe. The electrode interface was modified through a layer-by-layer (LBL) assembly strategy with dendrimer-stabilized Au nanoparticles (Au DSNPs) with high biocompatibility, nitrogen-doped carbon nanotubes (CNx) with excellent conductivity, and cell-targeting aptamers/antibodies with high specificity. Thus, targeted leukemia cells (HL-60 cells) could be captured specifically onto the nanoarchitected electrode surface while nontarget cells (K562 cells) could not be captured. Then, the electrochemical nanoprobe was further labeled onto the captured cells via the specific recognition ability of recombinant human tumor necrosis factor (TNF)-related apoptosis-inducing ligand (rhTRAIL) to the cognate death receptors DR4/DR5 expressed on the targeted cell surfaces. Since the electrochemical nanoprobe was fabricated through the combinative treatment of Au nanoparticle-

decorated magnetic Fe_3O_4 beads with rhTRAIL and horseradish peroxidase (HRP), an amplified electrochemical signal could be obtained with HRP-mediated catalytic oxidation reaction of thionine by H_2O_2 . Consequently, the sandwiched structure could be utilized for the detection of some specific types of leukemia cells and quantitative evaluation of DR4/DR5 expression level on these cells surfaces. An ultralow detection limit for leukemia cells as low as ~ 40 cells was achieved.

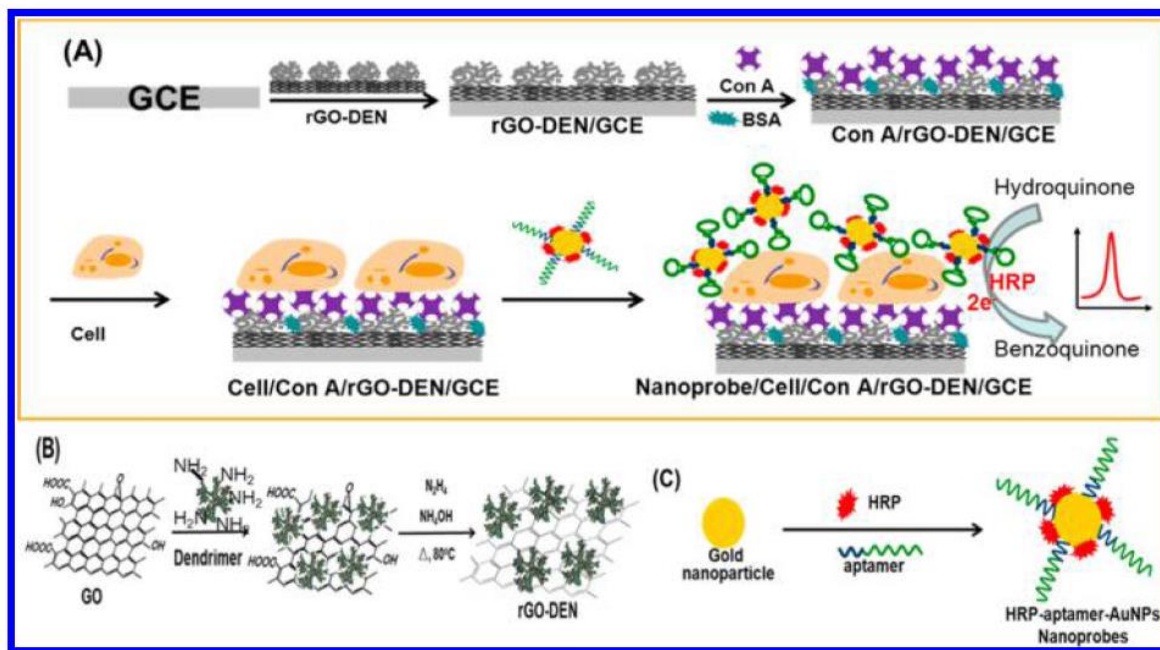


Figure 5. (A) Schematic illustration of the electrochemical aptamer biosensor for dynamic evaluation of cell surface N-glycan expression based on multivalent recognition and dual signal amplification, (B) Fabrication of PAMAM dendrimer-conjugated chemically reduced graphene oxide (rGO-DEN), and (C) Fabrication procedures of HRP- and aptamer-modified Au NP nanoprobe (HRP-Aptamer-AuNPs). Reprinted with permission from reference [38]. Copyright 2015 American Chemical Society.

With Con A-conjugated poly(amidoamine) dendrimer-modified reduced graphene oxide (rGO-DEN) as the sensing interface and HRP-aptamer-AuNPs as the nanoprobe, Li's group reported the electrochemical sensing of human acute lymphoblastic leukemia and evaluation of dynamic cell surface N-glycan expression (Figure 5) [38]. The rGO-DEN enhanced the electron transfer ability and improved the capture efficiency of target cells. The detection limit was as low as 10 cells/mL. Also, they presented a sandwich ECL biosensor by using Con A-integrating AuNPs modified $\text{Ru}(\text{bpy})_3^{2+}$ -doped silica nanoprobe (Au-RuSiO₂ NPs) for evaluating cell-surface N-glycan expression (Figure 6) [39]. The biosensor based on the effective ECL amplification of Au-RuSiO₂ NPs showed a detection range of $10^3 \sim 10^7$ cells/mL for K562 cells with a detection limit of 600 cells/mL. Intriguingly, the method can be used to evaluate cell-surface N-glycan expression by various external inhibitors and enzymes.

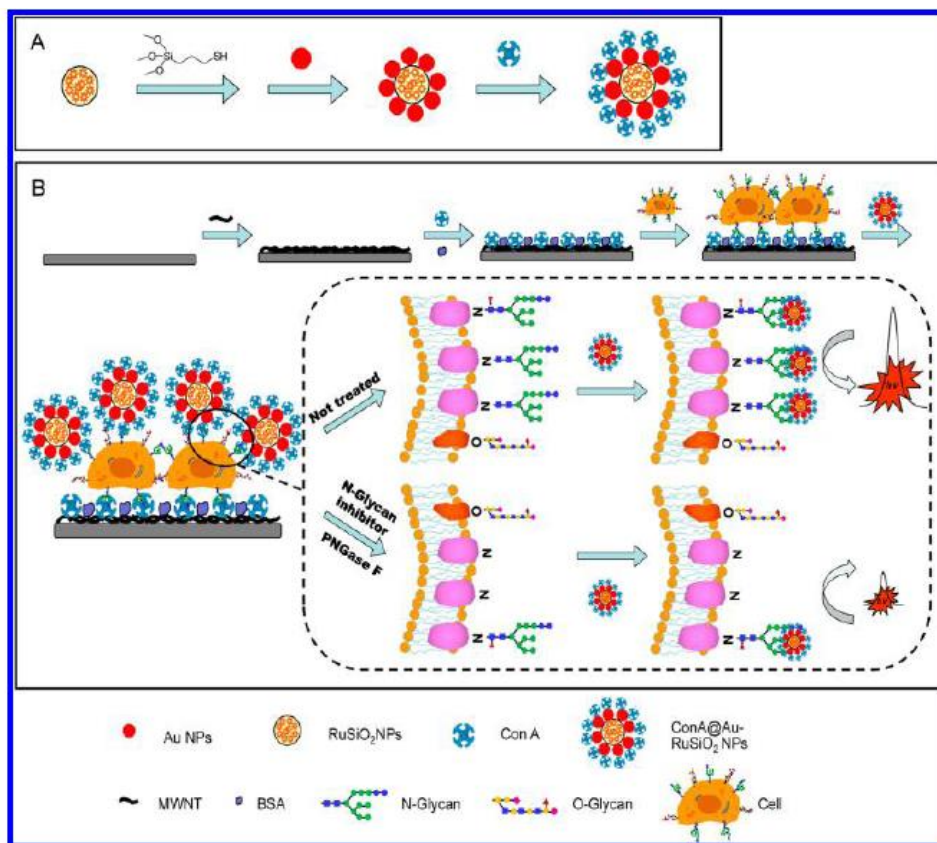


Figure 6. Schematic illustration of ECL biosensor for dynamic evaluation of cell surface N-glycan expression based on Con A: (A) fabrication procedures of Con A@Au–RuSiO₂ NPs and (B) ECL biosensor for cytosensing and evaluating cell surface N-glycan expression based on Con A@Au–RuSiO₂ NPs. Reprinted with permission from reference [39]. Copyright 2015 American Chemical Society.

Glycosylation of cell surfaces is of vital importance for many biological processes and related diseases. Ju's group reported the detection of cell glycan on the surface of K562 cells using ferrocene–concanavalin A (Fc-ConA) as the electrochemical probe and the recognition element [40]. A linear range of $10^4 \sim 10^7$ cells/mL was achieved with a detection limit of 3000 cells/mL was obtained. The average number of mannose group on single living K562 cell was determined to be 3.0×10^{10} . The value increased by 81% after treated by drugs. Zhang and coworkers reported the ECL detection of cell-surface carbohydrate expression using a nanoprobe Con A@Au/Ir-MSN, which was composed of Con A, luminescent Ir complex, mesoporous silica nanoparticles (MSN) and Au NPs (Figure 7) [41]. The luminescent Ir complex was loaded into the pores of MSN. Then, Au NPs were assembled onto the MSN surface to immobilization of large numbers of Con A molecules. In this work, the cells were immobilized on the electrode covered with poly(diallyldimethylammonium chloride) (PDDA)-functionalized graphene (PDDA/GR) and Con A. Zhang's group also reported that the peroxidase-like hemin/reduced graphene oxide/ gold nanorods (H-RGO-Au NRs) composite can be employed for the detection of cell-surface glycan expression (Figure 8) [42]. In this work, Con A anchored onto the electrode surface was used to immobilize the cells. Then, the Con A-modified H-RGO-Au NRs were attached onto the cell surface through the interaction of Con A and glycan. The H-RGO-Au NRs on

electrode surface catalyzed the reduction of H₂O₂.

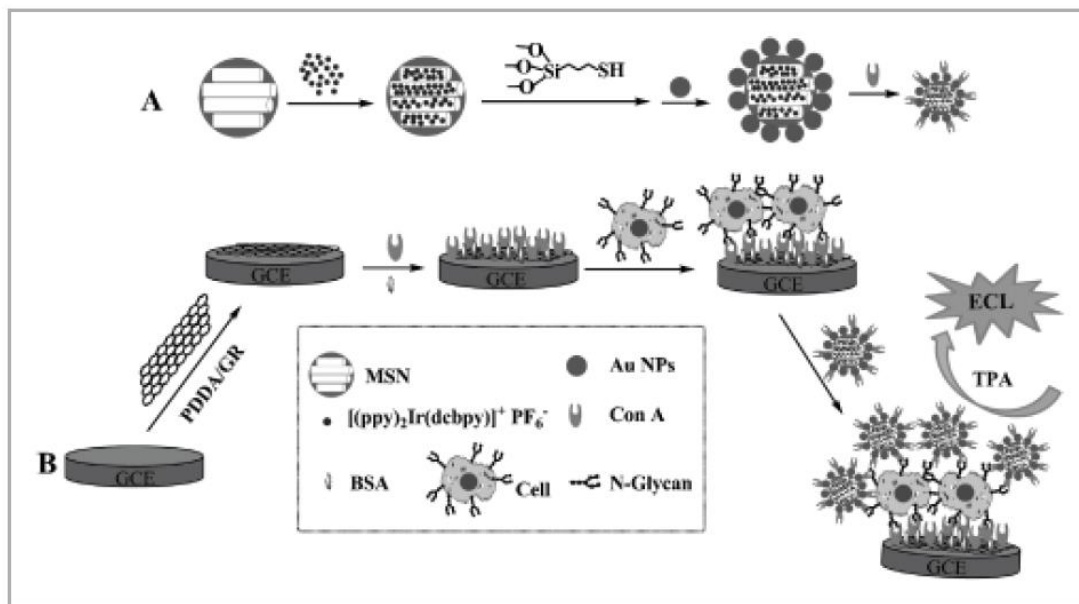


Figure 7. Schematic representation of: A) fabrication of the Con A@Au/Ir-MSN nanoprobe, and B) assembly of the electrode interface and the sandwich-like nanoarchitected electrode geometry for cytosensing and evaluating cell-surface N-glycan expression based on the Con A@Au/Ir-MSN nanoprobe. ppy: 2-phenylpyridyl; dcbpy: 4,4'-dicarboxy-2,2'-bipyridyl; BSA: bovine serum albumin; TPA: tripropylamine. Reprinted with permission from reference [41]. Copyright 2015 John Wiley and Sons.

With Con A-MWCNT and Con A-AuNPs as the sensing interfaces, Ju's group and Zhu' group reported the detection of cell glycan expression in response to drugs [43, 44]. EIS and optical microscope technique were used for monitoring the dynamic variation of glycan expression (Figure 9). Compared with the individual technology, the double-check mode increased the sensitivity and accuracy of the assay.

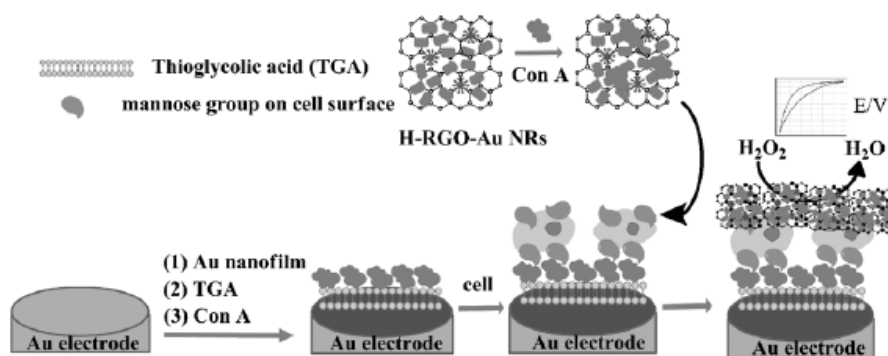


Figure 8. Procedure for cytosensing and the detection of glycan expression on K562 cell surface using the designed nanoprobe. Reprinted with permission from reference [42]. Copyright 2015 John Wiley and Sons.

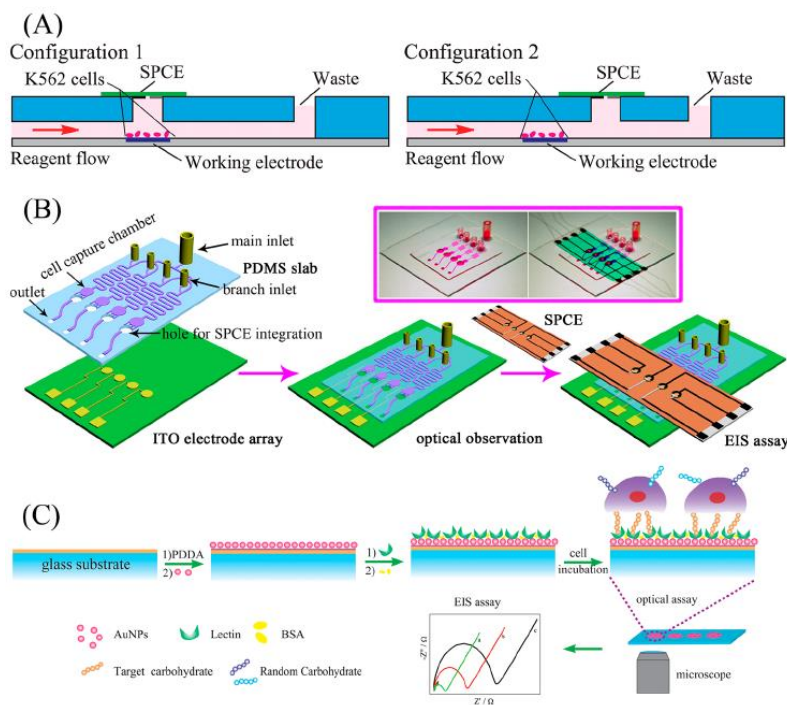


Figure 9. (A) Side view of one channel in the two microfluidic configurations. In configuration 1, the four circular openings of 3 mm diameter were punched on the four cell capture chamber regions of the PDMS slab for the SPCEs integrating. In configuration 2, the four circular openings of 3 mm diameter were punched in the down stream of the four cell capture chamber regions for the SPCEs integrating. (B) The construction process of the device for optical–electrochemical monitoring according to configuration 2. Inset shows photographs of the devices. (C) Schematic representation of lectin-based array for cell surface glycan evaluation. The recognition layer consisted of specific lectins which recognize the corresponding glycan on the cell surface. The EIS assay and optical microscopic observation were performed for the glycan evaluation. Reprinted with permission from reference [44]. Copyright 2015 American Chemical Society.

2.6 Cervical carcinoma cells

Cervical cancer is the second most prevalent cancer in women worldwide. Four major steps are involved in the development of cervical cancer, that is, the infection of metaplastic epithelium, viral persistence, appearance of cervical precancer, and invasion through the basement membrane of the epithelium [45]. Even though the development of cervical cancer takes even several decades, many women in less developed countries have been diagnosed due to the lack of effective screening systems [46]. If diagnosed with early-stage tumors, most women are likely to be cured along with long-term morbidity from treatment. Effective methods for determining tumor stages are preferred, a key factor for successful treatment of cervical cancer.

Li et al. utilized an electrochemical current rectifier (ECR) molecular device to construct a cytosensor for human cervical carcinoma (HeLa) cells detection [47]. For monolayer-based ECRs, 11-undecanethiol-1-ferrocene (UDT-Fc) and 16-mercaptohexadecanoic acid (MHDA) were firstly immobilized on the surface of a gold electrode which served as an electron transfer (ET) mediator and

insulating layer, respectively. After modification, a low redox current signal was observed due to the limited ferrocene molecules on the surface. The addition of K_2IrCl_6 as a redox probe, contributed to a cathodic current signal with higher magnitude while the anodic current vanished. In the negative potential sweep process, an obvious reduction potential of ferrocene was observed since the ferrocene could receive electrons from the working electrode. Thereby, an enhanced cathodic current occurred due to the fast transfer of electrons from the oxidized ferrocene to the iridate (IV) ions. However, the electron could not be transferred forward to iridate (III) ions resulting from the thermodynamical restriction during the reverse sweep. Thus, the anodic current was not detected. In the presence of HeLa cells, the folate (FA) molecules binding to MHDA recognize FA receptors rich in the surface of HeLa cells. As a result, HeLa cells could be immobilized on the FA-modified electrode, leading to a decreased peak current due to the electron transfer resistance of the cell membrane. A good linear relationship was obtained between electrochemical signals and HeLa cell concentration ranging from 10 to 10^6 cells/mL. Additionally, a low detection limit of 10 cells/mL was received even in the presence of normal cells HEK 293 cells.

Li and coworkers developed a novel electrochemical method for the detection of cell-surface glycan expression with human colon adenocarcinoma (LS180) cells as the models [48]. In their work, 5-hydroxy-3-hexanedithiol-1,4-naphthoquinone (JUGthio) was used as the electrochemical reporter. Specifically, the anti-selectin aptamers were immobilized on the electrode surface for the capture of selectin. The glycosylated LS180 cells competed with anti-selectin aptamers to bind with selectin. This resulted in a reduced oxidation signal of JUGthio. Thus, the glycosylation of cell surfaces could be determined easily and sensitively. The platform also allowed for the specific detection of LS180 cells in the range of 10^3 to 10^7 cells/mL.

2.7 Human Burkitt's lymphoma cells

Burkitt lymphoma is a common type of non-Hodgkin's lymphoma in which cancers occur in immune cells called B-cells in the germinal center [49]. One possible mechanism is that the immune system's response to Epstein-Barr is insensitive due to malaria, leading to the infected B-cells transferring into cancerous cells [50]. In Africa, young children infected with malaria and Epstein-Barr tend to be likely to be diagnosed with Burkitt lymphoma. As a fastest growing human tumor, Burkitt lymphoma causes an impaired immunity and fatal diseases if left untreated. However, intensive chemotherapy can be conducive to long-term survival in more than half the people with Burkitt lymphoma because of the quick spreading rate and prompt diagnosis [50].

Bi and coworkers demonstrated an electrochemiluminescence (ECL) assay for human Burkitt's lymphoma cells (Ramos) detection [51]. Firstly, magnetic Au- Fe_3O_4 nanoparticles are modified with two kinds of probes including aptamer (DNA2) and primer (DNA3) sequences through the interaction of Au-S. Then, the obtained toehold-aptamer/DNA primer/Au- Fe_3O_4 (TA/DP/Au- Fe_3O_4) nanoconjugates conjugated with DNA1-modified substrate through the hybridization of DNA1 with aptamer strand. After recognition of Ramos cells, the structure of aptamer in the functional

nanoconjugates changed, leading to these nanoconjugates transferring from the DNA1-modified substrate to the resulting supernatant.

Upon the introduction of DNA4, a strand displacement reaction (SDR) was initiated due to DNA4 complementary to the toehold DNA and aptamer, which resulted in separation of the nanoconjugates from targeted cells surface. In the presence of DNA polymerase and dNTPs, DNA3 in the released nanoconjugates could serve as a primer to initiate rolling circle amplification (RCA) with the aid of circular DNA template DNA5. The obtained long RCA products acted as an anchored platform for binding of numerous DNA6 labeled with ECL reactive molecules. By virtue of the magnetic properties, the resulting nanoconjugates can be easily trapped onto the surface of a magnetic Au electrode. Given the cascaded amplification, the fabricated ECL immunsensor could detect Ramos cells as low as 16 cells and even those spiked in complex samples and human blood samples.

Table 1. Comparison of the analytical properties of electrochemical techniques for the detection of cancer cells.

Cancer Cell	Method	Amplification strategy	Linear range (cells/mL)	Detection limit (cells/mL)	Refs.	
Lung	CA	hydrazineAuNPs	15–10 ⁶	8	[13]	
	DPV	HPR/MWCNT	20–4×10 ⁵	10	[14]	
Breast	SWV	CdS	10 ⁴ –10 ⁷	3.3×10 ²	[16]	
	ASV	Apt-Qdots	10 ² –10 ⁶	100	[20]	
	ASV	CdS or PbS nanocrystals	10 ² –10 ⁶	100	[21]	
	SWV	MBs/QDs/SiO ₂ NPs	250–10 ⁴	85	[22]	
	IT	HCR/HRP	–	4	[23]	
	SWV	RCA	20–5×10 ⁶	12	[24]	
	SWV	Ag NCs	50–5000	50	[25]	
Colorectal	DPV	AuNPs/Silver	500–10 ⁶	100	[26]	
	ECL	CQDs/SiO ₂ NPs	500–2×10 ⁷	230	[52]	
	EIS	AuNPs	10–10 ⁶	2	[30]	
	Liver	EIS	–	10 ² –10 ⁶	2	[31]
		DPV	–	1–14	5	[34]
	DPV	MWCNT/Th/AuNPs	50–5×10 ⁶	20	[15]	
	Leukemia	CV	Au DSNPs/CN _x	10 ³ –10 ⁶	40	[36]
DPV		rGO–DEN/HRP-aptamer-AuNPs	10 ² –10 ⁴	10	[38]	
ECL		Au–RuSiO ₂ NPs	10 ³ –10 ⁷	600	[39]	
DPV		ferrocene	10 ⁴ –10 ⁷	3000	[40]	
CV		H-RGO-Au NRs	50–800	10	[42]	
ECL		Con A@Au/Ir-MSN	10 ² –10 ⁶	100	[41]	
EIS		MWCNT	10 ⁴ –10 ⁷	50	[43]	
Carcinoma	ECL	PtNPs/CNTs	500–5.0×10 ⁶	500	[53]	
	DPV	K ₂ IrCl ₆	10–10 ⁶	10	[47]	
	DPV	–	10 ³ –10 ⁷	–	[48]	
Lymphoma	ECL	RCA	20–500	16	[51]	

3. CONCLUSION

It has been shown that various electrochemical techniques can be utilized for the fabrication of sensitive biosensors for cancer cells detection. Their analytical performances have been summarized and compared, as shown in Table 1. Significant advances have been made in past decades with different functional nanostructured biomaterials flourishing. Pursuing more multifunctional materials or bioenzymes for advancing the progress of electrochemical sensors for cancer cells assay is never stopped. By virtue of new developments in custom engineering of biorecognition components, more and more new reliable and early stage biomarkers are discovered, which boosts the development of electrochemical sensors for more cancer cells detection. Additionally, there is still much effort needed to make for simultaneous measurement of various cancer cells in a short period of time. The integration of electrochemical sensors into a portable device for the sensitive detection of cancer cells needs to be extensively explored in the future. In comparison with the current analytic systems, the development of these systems would also contribute to promising progress in terms of simplicity, speediness, cost, and automation.

ACKNOWLEDGMENTS

Partial support of this work by the National Natural Science Foundation of China (21305004), the Joint Fund for Fostering Talents of National Natural Science Foundation of China and Henan Province (U1304205) and the Science & Technology Foundation of Henan Province (17A150001) is gratefully acknowledged.

References

1. A. B. Chinen, C. M. Guan, J. R. Ferrer, S. N. Barnaby, T. J. Merkel and C. A. Mirkin, *Chem. Rev.*, 115 (2015) 10530.
2. D. Hanahan and R. A. Weinberg, *Cell*, 144 (2011) 646.
3. M. F. Ullah and M. Aatif, *Cancer Treat. Rev.*, 35 (2009) 193.
4. H. Kobayashi and P. L. Choyke, *Accounts Chem. Res.*, 44 (2011) 83.
5. J. Liu, Y. Qin, D. Li, T. Wang, Y. Liu, J. Wang and E. Wang, *Biosens. Bioelectron.*, 41 (2013) 436.
6. S. Xu, J. Liu, T. Wang, H. Li, Y. Miao, Y. Liu, J. Wang and E. Wang, *Talanta*, 104 (2013) 122.
7. K. Wang, M. Q. He, F. H. Zhai, R. H. He and Y. L. Yu, *Talanta*, 166 (2017) 87.
8. L. S. Hu, S. Q. Hu, L. Y. Guo, C. C. Shen, M. H. Yang and A. Rasooly, *Anal. Chem.*, 89 (2017) 2547.
9. J.-Y. C. Hye-Jin Sung, *BMB reports*, 41 (2008) 615.
10. S. K. Arya and S. Bhansali, *Chem. Rev.*, 111 (2011) 6783.
11. P. J. Mazzone, J. Hammel, R. Dweik, J. Na, C. Czich, D. Laskowski and T. Mekhail, *Thorax*, 62 (2007) 565.
12. J. N. Arnold, R. Saldova, M. C. Galligan, T. B. Murphy, Y. Mimura-Kimura, J. E. Telford, A. K. Godwin and P. M. Rudd, *J. Proteome Res.*, 10 (2011) 1755.
13. T. A. Mir, J.-H. Yoon, N. G. Gurudatt, M.-S. Won and Y.-B. Shim, *Biosens. Bioelectron.*, 74 (2015) 594.
14. X. Zhang, W. Lu, J. Shen, Y. Jiang, E. Han, X. Dong and J. Huang, *Biosens. Bioelectron.*, 74 (2015) 291.

15. X. Zhang, C. Huang, Y. Jiang, J. Shen, P. Geng, W. Zhang and Q. Huang, *RSC Adv.*, 6 (2016) 112981.
16. T. Li, Q. Fan, T. Liu, X. Zhu, J. Zhao and G. Li, *Biosens. Bioelectron.*, 25 (2010) 2686.
17. K. D. Miller, R. L. Siegel, C. C. Lin, A. B. Mariotto, J. L. Kramer, J. H. Rowland, K. D. Stein, R. Alteri and A. Jemal, *CA-Cancer J. Clin.*, 66 (2016) 271.
18. Q. Shen, J. J. Rahn, J. Zhang, N. Gunasekera, X. Sun, A. R. Shaw, M. J. Hendzel, P. Hoffman, A. Bernier and J. C. Hugh, *Mol. Cancer Res.*, 6 (2008) 555.
19. J. C. B. Jezersek, Z. Rudolf, S. NovakoviCa, *Cancer Letters*, 110 (1996) 137.
20. J. Li, M. Xu, H. Huang, J. Zhou, E. S. Abdel-Halimb, J.-R. Zhang and J.-J. Zhu, *Talanta*, 85 (2011) 2113.
21. S. Lv, Y. Guan, D. Wang and Y. Du, *Anal. Chim. Acta*, 772 (2013) 26.
22. X. Hua, Z. Zhou, L. Yuan and S. Liu, *Anal. Chim. Acta*, 788 (2013) 135.
23. G. Zhou, M. Lin, P. Song, X. Chen, J. Chao, L. Wang, Q. Huang, W. Huang, C. Fan and X. Zuo, *Anal. Chem.*, 86 (2014) 7843.
24. Q. Sheng, N. Cheng, W. Bai and J. Zheng, *Chem. Commun.*, 51 (2015) 2114.
25. Q. Guo, X. Li, C. Shen, S. Zhang, H. Qi, T. Li and M. Yang, *Microchim. Acta*, 182 (2015) 1483.
26. J.-J. Zhang, F.-F. Cheng, T.-T. Zheng and J.-J. Zhu, *Biosens. Bioelectron.*, 89 (2016) 937.
27. S. J. Clarke, C. S. Karapetis, P. Gibbs, N. Pavlakis, J. Desai, M. Michael, N. C. Tebbutt, T. J. Price and J. Tabernero, *Crit. Rev. Oncol. Hemat.*, 85 (2013) 121.
28. R. L. Siegel, K. D. Miller and A. Jemal, *CA-Cancer J. Clin.*, 65 (2015) 5.
29. H. Kelly and R. M. Goldberg, *J. Clin. Oncol.*, 23 (2005) 4553.
30. A. B. Hashkavayi, J. B. Raoof, R. Ojani and S. Kavosian, *Biosens. Bioelectron.*, 92 (2017) 630.
31. L. Kashefi-Kheyrabadi, M. A. Mehrgardi, E. Wiechec, A. P. F. Turner and A. Tiwari, *Anal. Chem.*, 86 (2014) 4956.
32. D. Shangguan, L. Meng, Z. C. Cao, Z. Xiao, X. Fang, Y. Li, D. Cardona, R. P. Witek, C. Liu and W. Tan, *Anal. Chem.*, 80 (2008) 721.
33. P. A. Farazi and R. A. DePinho, *Nat. Rev. Cancer*, 6 (2006) 674.
34. L. Qu, J. Xu, X. Tan, Z. Liu, L. Xu and R. Peng, *ACS Appl. Mater. Interfaces*, 6 (2014) 7309.
35. B. W. Futscher, J. Nordlund, L. Milani, A. Lundmark, G. Lönnerholm and A.-C. Syvänen, *PLoS ONE*, 7 (2012) e34513.
36. T. Zheng, J. J. Fu, L. Hu, F. Qiu, M. Hu, J. J. Zhu, Z. C. Hua and H. Wang, *Anal. Chem.*, 85 (2013) 5609.
37. M. Su, L. Ge, Q. Kong, X. Zheng, S. Ge, N. Li, J. Yu and M. Yan, *Biosens. Bioelectron.*, 63 (2015) 232.
38. X. Chen, Y. Wang, Y. Zhang, Z. Chen, Y. Liu, Z. Li and J. Li, *Anal. Chem.*, 86 (2014) 4278.
39. Z. Chen, Y. Liu, Y. Wang, X. Zhao and J. Li, *Anal. Chem.*, 85 (2013) 4431.
40. Y. Xue, L. Ding, J. Lei and H. Ju, *Biosens. Bioelectron.*, 26 (2010) 169.
41. H. Zhou, Y. Yang, C. Li, B. Yu and S. Zhang, *Chem. Eur. J.*, 20 (2014) 14736.
42. J. Liu, X. Xin, H. Zhou and S. Zhang, *Chem. Eur. J.*, 21 (2015) 1908.
43. Y. Xue, L. Bao, X. Xiao, L. Ding, J. Lei and H. Ju, *Anal. Biochem.*, 410 (2011) 92.
44. J.-T. Cao, X.-Y. Hao, Y.-D. Zhu, K. Sun and J.-J. Zhu, *Anal. Chem.*, 84 (2012) 6775.
45. M. Schiffman, P. E. Castle, J. Jeronimo, A. C. Rodriguez and S. Wacholder, *Lancet*, 370 (2007) 890.
46. S. E. Waggoner, *Lancet*, 361 (2003) 2217.
47. H. Li, D. Li, J. Liu, Y. Qin, J. Ren, S. Xu, Y. Liu, D. Mayer and E. Wang, *Chem. Commun.*, 48 (2012) 2594.
48. Z. Shao, Y. Li, Q. Yang, J. Wang and G. Li, *Anal. Bioanal. Chem.*, 398 (2010) 2963.
49. D. Burkitt, *Brit. J. Surg.*, 46 (1958) 218.
50. E. M. Molyneux, R. Rochford, B. Griffin, R. Newton, G. Jackson, G. Menon, C. J. Harrison, T. Israels and S. Bailey, *Lancet*, 379 (2012) 1234.

51. M. Chen, S. Bi, X. Jia and P. He, *Anal. Chim. Acta*, 837 (2014) 44.
52. M. Su, H. Liu, L. Ge, Y. Wang, S. Ge, J. Yu and M. Yan, *Electrochim. Acta*, 146 (2014) 262.
53. L. Ge, M. Su, C. Gao, X. Tao and S. Ge, *Sens. Actuat. B: Chem.*, 214 (2015) 144.

© 2017 The Authors. Published by ESG (www.electrochemsci.org). This article is an open access article distributed under the terms and conditions of the Creative Commons Attribution license (<http://creativecommons.org/licenses/by/4.0/>).